Cytotoxic Effect of Free and Immobilized Elastase from Klebsiella Pneumoniae In Vitro And In Vivo

Jawad N. K. Makassees[1], Neihaya H. Zaki[2]*, Asmaa, A. Hussein[3]
[1] Directorate of Education Governate, Wasit, Iraq
[2] Department of Biology, College of Science, Mustansiriyah University, Baghdad /Iraq
[3] Department of Molecular and Medical Biotechnology, College of Biotechnology, Al-Nahrain University, Jadriya, Baghdad /Iraq
jawadnk1983@gmail.com
E-mail: dr.neihayahz@uomustansiriyah.edu.iq

Abstract
Forty-eight of Klebsiella pneumoniae isolates were collected from different sources in hospitals of Wasit Governorate. The isolate represents a potential source of elastase enzyme. Elastase was purified by three steps of ammonium sulfate precipitation, ion-exchange chromatography, and gel-filtration chromatography. The optimal temperature and pH for elastase were 37 C and 7 respectively, and its stable on the same conditions. The activity of this elastase was found to decrease when the temperature was higher than 40 C, and also inhibited by ZnCl2, FeCl2, and MnCl2 ions. Immobilized elastase on TiO2 NPs, showed low cytotoxicity to normal cell line in vitro, but it had anti-cancer activity against A375 cancer cell line and showed high significant against it within IC50 of (92.48, 78.16) for free and immobilize elastase respectively. High Content Screening provides multiparametric study of chemical toxicity at the cancer cells. In addition, immobilized elastase was low cytotoxicity when used it in vivo.
Keywords: Klebsiella pneumoniae, Elastase, Immobilization, TiO2-Nps- Cytotoxicity- In Vivo, Anticancer, High Content Screening.

1. Introduction

Klebsiella pneumoniae is a non-motile member of the Enterobacteriaceae (Vasaikar et al., 2017). It is a Gram-negative rod shape, facultatively anaerobic, lactose fermenter with a prominent capsule bacillus, which is ubiquitously present in the environment such as vegetation, water, soil and readily isolated from mammalian mucosal surfaces (Calbo & Garau, 2015).
Elastase is an enzymes from a class of proteases that break down, degrade elastin. an elastic fiber that, together with collagen, determine the mechanical features of connective tissue (Everett & Davies, 2021). Elastase's proteolytic action is not limited to elastin. They can assault any soluble protein with proper, surface-exposed amino acid sequences. Elastase, for example, breaks down tropoelastin, a soluble elastin precursor (Heinz, 2020). Immobilization process is to optimize the operational performance of an enzyme for industrial applications (Meryam Sardar, 2015).
Cytotoxicity is a multifaceted process that affects several variables and pathways. These parameters are cellular organelles whose activity varies as a result of drug-induced apoptosis and necrosis. . Good examples of cytotoxicity factors are nuclear morphology, cell permeability, and mitochondrial function, which results in the loss of mitochondrial membrane potential and the release of cytochrome C from mitochondria. (Karanam & Arumugam, 2020).
Cancer is an abnormal and random growth of cells arising from a single cell that has a disrupted regulatory mechanisms (Povoa et al., 2021). whose growth outpaces and is uncoordinated with that of the normal tissue of its origin, and which remains in the same excessive manner after the stimuli that elicited the changes have been removed (Kruchko et al., 2019). The aim of this study was purification and characterization of elastase enzyme from K. pneumoniae and determine the cytotoxicity of free and immobilized elastase in vitro and in vivo.

2. Material and Methods

Klebsiella pneumoniae identification

About 163 samples were collected from different clinical sources in Wasit hospitals. Identification of K. pneumoniae was done by culturing on McConkey agar (Patel et al., 2017), and confirmed by Polymerase chain reaction (PCR) with 16S rRNA (Data not shown) (Abbas et al., 2020).

Elastin preparation

Mature sheep lung tissues are completely and thoroughly washed with distil water and autoclaved with(20) volumes distilled water at(1) atmosphere for (45) minutes in a container fitted with a loose-fitting gauze plug. The autoclave step is repeated with fresh distilled water until no further protein is detected in the supernatant. The residue is dried in room temperature after treatment with ethanol. Then the remainder is ground to form an elastin powder (Logan, 2014).

Screening of elastase production

Quantitative Assay was used for detection of

doi.org/10.31838/hiv23.03.77 Received: 05.10.22, Revised: 02.11.22, Accepted: 04.12.22.

Elastase production from 48 isolates of *K. pneumoniae* as mentioned in (Li *et al.*, 2019).

Purification of Elastase

Elastase was extracted from *K. pneumoniae* (NJ22) supernatant as mentioned in (Lei *et al.*, 2018). Partial purified by ammonium sulfate precipitation at concentration (20-90 %), then DEAE-cellulose column and Sephadex G-150 column were used for further purification of the enzyme (Shinji *et al.*, 2019)

Elastase characterization

pH effects on elastase activity and stability of enzyme were measured at range of (5 to 10). Also, temperature effects on elastase activity and stability were measured at different temperatures (30, 35, 40, and 45) °C. With various salts, the impact of various inorganic ions on enzyme activity was studied. ($MgCl_2$, $CaCl_2$, KCl_2 , $MnCl_2$, $FeCl_2$ and $ZnCl_2$) at concentrations (5mM). After measuring the enzyme activity, the results were provided as a percentage of the original activity (%) (Lei *et al.*, 2018).

Immobilization of elastase on TiO2 nanoparticles

Adsorption of elastase on TiO2 nanoparticles was done by method mentioned in (Ahmad & Sardar, 2014), and characterization of the immobilization was done with AFM analysis.

Cytotoxicity effect of free and immobilized elastase *in vitro*

Cytotoxicity analysis on normal cell line (HdFn) and cancer cells line (A375) by MTT-assay with different concentrations of free and immobilize elastase 12.5,25,50,100, 200 and 400 µg/mL (Hu *et al.*, 2020). The cell livability could be evaluated as follows (Al-Dulimi *et al.*, 2020):

Total Cell Count mL-1 = Cell count x Dilution Factor (Sample Volume) x 10^4

High Content Screening (HCS) of elastase on A375 cell line

High content screening is a powerful tool employs fluorescence indicator to define cellular morphology and molecular response to compounds treatment via measuring five orthogonal cell health parameters *in vitro*. The parameters were: viability cell count, total nuclear intensity, cell membrane permeability, mitochondrial membrane permeability and cytochrome C. The Procedure is described in detail by (Abraham *et al.*, 2008).

Cytotoxicity assay of free and immobilized elastase *In vivo*

Fifty healthy mature mice were used in this experiment. Their age was in the range 6-8 weeks old, and their weight was around 25-30 g. They were divided randomly into ten groups and five mice were kept in each cage (Cookson & Stirk, 2019). Group1: (Intraperitoneal injected normal slain and served as control). Group2: (injected IP with TiO2 nanoparticles as dose 0.3mg/ml /day for 7 days). Group 3: (injected TiO2 nanoparticles as dose 0.4mg/ml /day for 7 days). Group 4: (injected TiO2 nanoparticles as dose 0.5mg/ml /day for 7 days). Group 5:(injected IP elastase as dose 0.3mg/ml /day for 7 days). Group 6: (injected elastase as dose 0.4mg/ml /day for 7 days). Group 7: (injected elastase as dose 0.5mg/ml /day for 7 days). Group8: (injected immobilized elastase IP with TiO2- NPS as dose 0.3mg/ml /day for 7 days). Group 9: (injected immobilized elastase with TiO2-NPS as dose 0.4mg/ml /day for 7 days). Group 10: (injected immobilized elastase with TiO2-NPS as dose 0.5mg/ml /day for 7 days).

Histopathological Study

At the end of experiments, the animals were sacrifice. The specimens were taken from the liver, lung, spleen and kidney. The tissues were preserved in 10% formaldehyde immediately after removal. Histopathological section prepared and stained according to (Luna, 1968 and Crissman *et al.*, 2004).

3. Results and discussion

Morphological Characteristics of *K pneumoniae*

In Table (1), 48 isolates (29.44%) were successfully diagnosed as K. pneumoniae and appeared mucoid, large, and pink on MacConkey agar due to lactose fermenting (Yu et al., 2007).

Table (1): *K. pneumoniae* isolated from different clinical sources

Number (%) of K.pneumoniae	Number of specimens	Isolaton source
10	37	Sputum
14	42	Urine
9	24	Wound
2	14	Ear
6	20	Pharynx
7	23	Burn
48 (29.44)	163	Total

Screening of elastase production

All K. pneumoniae isolates could generate the enzyme with specific activities ranging (0.003-1.613) U/mg protein, and (NJ22) isolate had the highest specific activity of 1.613 U/mg protein.

Purification of elastase

Elastase saturation was 60% as best precipitation of enzyme when ammonium sulfate was applied to the crude enzyme (supernatant). The result of purification appeared in Table (2). Results showed that elastase activity and the best enzyme specific activity(U/mg protein), was measured to be 36 and 96 U\mg protein.

Table (2): Purification steps for elastase produced by *K. pneumoniae* (NJ22)							
Purification step	Volume (ml)	Enzyme activity (U/ml)	Protein concentration (mg/ml)	Specific activity (U/mg protein)	Total activity (U)	Purification (folds)	Yield (%)
Crude enzyme	75	2.6	0.6	4.4	195	1	100
Ammonium sulphate precipitation 60%	20	10	0.5	20	200	4.5	102.5
DEAE-cellulose	18	8.3	0.23	36	149.4	8.2	76.6
Sephadex G150	15	9.6	0.1	96	144	21.8	73.8

The results showed that protein with 76.6 % overall yield and 8.2 purification fold after purification by DEAE cellulose. On the basis of their affinity for the ion exchanger, ion chromatography separates ions and polar compounds. It operates on large proteins, tiny nucleotides, and amino acids, among other charged molecules. However ion chromatography must be done in conditions that are one unit away from the isoelectric point of a protein (Din et al., 2021). Specific activity 170 U/mg with purification folds 39.2 U/mg and(8.8%) overall yield time of elastase purified from P. aeruginosa recorded by (Kotb et al., 2019).

Characterizations of purified elastase

Effects of PH on elastase (Activity and stability)

The enzyme increased in activity from pH 6 to 8, however, maximum elastase activity was observed at pH 7-8. After incubation of elastase for 30 min in rang of pH the enzyme showed the maximum stability in pH 7 with maximum remaining activity (100 %) (Figure:1).

(Fujii et al., 2020) reported that the optimum elastase activity at pH 8) is produced by Streptomyces bacteria. According to (Bisswanger, 2014), pH can affect enzyme activity in a variety of ways, including ionization of groups in the substrate and ionization of groups in the enzyme's active site. In high acidic or basic solutions, most enzymes can be irreversibly denaturized (Mukherjee & Banerjee, 2006).

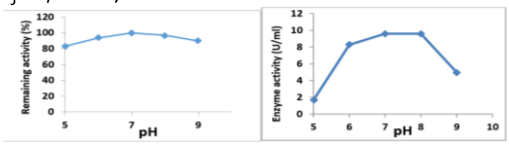

Figure (1): Effects of pH at (activity and stability) of pure elastase

Effect of Temperature on elastase Activity and stability

Elastase activity was assayed at temperatures ranged from 30 to 45 C°, enzyme activity was obtained at 35 to 40 C° and the maximum at 37c, with observed decreases in activity of higher or low temperatures of incubations. While heat stability demonstrated that the enzyme maintained 100% of its activity when incubated at 35°C (Fig. 2).

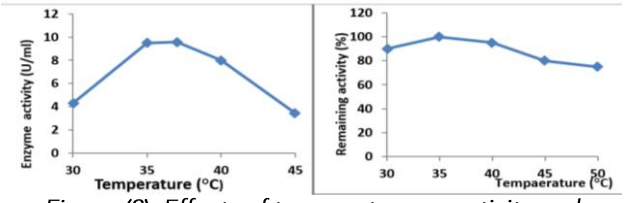

Figure (2): Effects of temperature on activity and stability of purified elastase

The reactant molecules have more kinetic energy as the temperature rose, leading to more efficient collisions per unit of time, but this should be done while preserving the intact and proper configuration of the tertiary structure of an enzyme (Dong *et al.*, 2018). we agree with study submitted by (Lei *et al.*, 2018) they mentioned the higher activity of elastase at temperature 37°C produce from *Chryseobacterium indologenes.*

Effect of Ions and Inhibitors on elastase Activity

The results showed that Mgcl2, CaCl2 and KCl at 5mM concentration very slight affect enzyme activity, but MnCl2 was show to inhibit enzyme activity to 53%, FeCl2 inhibit 80% and ZnCl2 75% of enzyme activity, Table (3).

Table (3): Metal ions and inhibitors effect on elastase activity		
Reagent	Concentration (mM)	Remaining activity (%)
Control (Enzyme)		100
MgCl2	5	99.1
CaCl2	5	97
KCl	5	88.5
MnCl2	5	47
FeCl2	5	19.3
ZnCl2	5	25.1

(Lei et al., 2018) showed that elastase purified from Chryseobacterium indologenes have little effect to enzyme activity by CaCl2 and KCl lost about 14 % from its activity, while the enzyme activity increased when use MgCl2, but there is a sharp effect by MnCl2 ,FeCl2 and ZnCl2 .

Anticancer activity of purified free and immobilize elastase

Table (4) showed the concentration of the elastase enzyme is increased, which decreases the viability of the cells. The decreasing of A375 cells viability was noted at 400 µg /ml (59.11 ± 5.54) .While the maximum A375 cell viability was (95.41±1.41) at

12.50 µg/ml, and cell viability ranged from (95.18 ± 1.28 to 36.36 ± 3.04) from 12.50 to 400 µg/ml show in table (4).

Table (4): Cytotoxicity effect of free and immobilize elastase on A375 and HdFn				
Concentration µg mL-1	Mean Inhibition of cell viability (%) ± SD			
	Elastase on A375	Elastase on HdFn	elastase +TiO2 on A375	elastase +TiO2 on HdFn
400	59.11 ± 5.54	81.29 ± 1.41	36.36 ± 3.04	74.79 ± 4.22
200	63.70 ± 2.12	89.27 ± 2.45	46.10 ± 4.69	87.25 ± 6.11
100	75.31 ± 4.15	92.21± 0.47	58.79 ± 9.59	93.60 ± 2.10
50	88.27 ± 2.57	95.72 ± 0.64	78.74 ± 7.03	96.49 ± 2.68
25	94.79 ± 1.33	95.41 ± 1.14	95.72 ± 0.81	93.81 ± 312
12.50	95.41± 1.41	93.90 ± 2.75	95.18 ± 1.28	98.65 ± 4.05

(Figure:3) showed that elastase with an IC50 value of 92.48 µg/ml, the enzyme demonstrated significantly the most potent cytotoxic activity. However, the action of elastase on the HdFn normal cell line resulted in an IC50 of 384.5 µg/ml. With an IC50 value of 78.16 µg/ml, the immobilize elastase demonstrated noticeably the most powerful cytotoxic effect. However, the effect of immobilize elastase on the HdFn normal cell line led to an IC50 of 655.0 µg/ml.

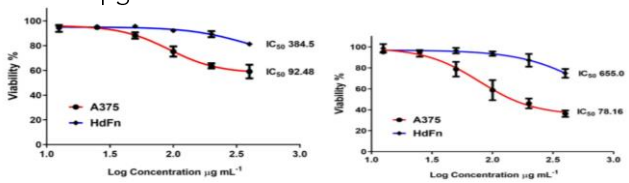

Figure (3): IC_{50} effect of free and immobilized elastase on A375 and HdFn cells

Various enzyme doses, ranging from 12.50 to 400 µg/ml, were used in the MTT Assay to determine the cell viability and inhibition rate on the cancer cell line. In comparison to a normal cell line(HdFn), the treated cells' percentage of viability was calculated. (Sharma and Ratain, 2015).

Multi-parameters cytotoxic activity of elastase on A375 cell line

The viability of the A375 cell line was considerably impacted by the purified elastase, as shown by the viable cell count data reported in table (5), which decreased to(2123±102.5)cells at 200µg/ml and (3338±441.2) at 100 µg/ml. While a viability for the other doses was 3451±106.1 and 3431±18.38 when compared to control for 50µg/ml and 25µg/ml, respectively, It did not distinguish itself much from the control.

Table (5): Cytotoxicity effect of immobilize elastase on viable cells count					
Treatment (µg mL-1)	HCS Parameters (mean ± SD)				
	VCC	TIN	CMP	MMP	CC
Untreated	3411 ±162.6	455.5±6.364	139.5±14.85	552.5 ±34.65	422.5 ± 24.42
200	2123 ±102.5	622.5±16.26	171.5±16.16	331.0 ±22.63	615.0 ± 29.70
10	3338 ±441.2	536.5±16.26	151.5±20.51	426.5 ±6.364	516.5 ± 34.65
50	3451 ±106.1	437.5±38.89	141.0±9.899	505 ± 25.46	418.5 ± 9.192
25	3431 ±18.38	423.0±50.91	140.0±11.31	568 ± 25.46	418.5±42.43
*Different letters: significant differences between mean ($p < 0.05$) "Viable cell count (VCC), nuclear intensity (NI), cell membrane permeability (CMP), mitochondrial membrane potential (MMP) and cytochrome C"					

In table (5) purified elastase demonstrates a considerable increase in the A375 cell line's nuclear intensity, this rise was dose-related. The highest percentage of increasing was 622.5±16.26 at 200µg/ml when compared with control. Significant characteristics of the cell's apoptotic morphology include aggregation, nuclear condensation, nuclear fragmentation, cell shrinkage, and the development of apoptotic bodies. (Crowley et al., 2016).

On the other hand, the mitochondrial membrane potential (MMP) data in Table (3-3) shows that the MMP dramatically decreased at 200 µg/ml and 100 µg/ml. Apoptosis is frequently disrupted during cancer growth, and it is critical to initiate correct apoptosis. This is brought on by mitochondrial outer membrane permeabilization (MOMP), which in turn causes the activation of caspase and the destruction of protein substrates (MOMP pathway) (Al-Dulimi et al., 2020)

Also, cell membrane potential (table: 5) showed that 200 µg/ml has no significantly increased CMP 171.5±26.16 when compared with control. Loss of cell membrane integrity is a frequent phenotypic characteristic of severe cytotoxicity, and changes in cell membrane permeability have been associated to toxic and apoptotic events. (Al-shukri et al., 2020).

Results for cytochrome C release in table (5) showed that, in comparison to the control, cytochrome C release increased dramatically when concentration increased by 200 µg/ml. With quantitative measurements of numerous parameters related to toxicity, the high content screening test is considered a predictive assay for monitoring morphological changes in cells due to toxic effect.(Ma et al., 2017).

Cytotoxicity assay *in vivo*

The sections of liver in control groups were showed normal appearances of hepatic lobules, hepatic cords and cytoarchetecture of live cellular composites Figure (4- A). The sections of liver were similar those in control groups when used elastase at concentration (0.3,0.4,0.5 mg/ml) normal

appearance of central vein, hepatocyte, sinusoid and kupffer cells figure(4- B). However the sections of the liver showed normal appearance when used TiO2NPs at (0.3,0.4)mg/ml while show mild zonal degenerative changes that characterized by mild cellular selling, vacular degeneration and nuclear hypertrophy when used higher concentration (0.5) mg/ml of NPs figure(4- C). When injection the elastase immobilized with TiO2 NPs at concentration (0.3) mg/ml , the sections of the liver showed normal appearance but when used (0,4,0.5) mg/ml of the liver showed marked disarrangement of hepatic cords with moderate hepatitis characterized by infiltration of leukocytes mainly lymphocyte with marked vacular degeneration and necrosis of hepatocytes figure(4-D).

The sections of splenic white and red pulp in control groups also showed lymphocyte, macrophage and sinus normal appearances figure (5- A). The sections of spleen was showed white pulp and red pulp similar those in control groups when used elastase at concentration (0.3, 0.4, 0.5) mg/ml figure (5- B). When injection the mice by TiO_2 NPs with concentration (0.3, 0.4, 0.5) mg/ml ,shows lymphocytes, sinusoids and megakaryocytes sections of splenic was similar those in control groups figure (5- C). The section of spleen when used elastase immobilized on TiO_2 NPs at concentration (0.3, 0.4) mg/ml ,showed normal appearance as control groups while at high concentration (0.5) mg/ml showed peripheral zone depletion with amyloid deposition associated with atrophy of white pulp and vaculated lymphocytes figure (5- D).

The sections of renal cortex and medulla in control groups also showed normal appearances normal thick segment and collecting renal tubule figure (6- A). The sections of kidney showed normal glomeruli, collecting, proximal and distal convoluted tubules was similar those in control groups when injection mice intraperitoneally by elastase at concentration (0.3, 0.4, 0.5) mg/ml figure (6- B). The sections of renal cortex showed normal appearance in used TiO_2 NPs at concentration (0.3, 0.4) mg/ml, but showed at concentration (0.5) mg/ml of TiO_2 NPs mild vacular and granular degeneration of epithelial cells of renal tubules with normal cytoarchetecture of renal tubules of renal medulla figure (6- C). The section of renal medulla when used elastase immobilized on TiO_2NPs showed normal appearance at concentration (0.3, 0.4) mg/ml while showed moderate vacular degeneration and swelling of epithelial renal tubules at (0.5) mg/ml of elastase immobilized on TiO_2 NPs figure (6- D).

The sections of lung also showed terminal bronchiole, alveolus and pnumocyte-I and type-II a normal appearances pulmonary air spaces and pulmonary passages in control groups figure (7- A). The sections of lung was similar those in control groups when injection the mice intraperitoneally by elastase only at concentration (0.3, 0.4, 0.5) mg/ml figure (7- B). The sections of lung when used only TiO2 NPs at concentration (0.3, 0.4, 0.5) mg/ml was showed normal alveolus, pnumocyte-I and type-II were similar those in control group figure (7- C). The sections of lung was showed normal bronchiole, alveolus, pnumocyte-I and type-II similar those in control group when used elastase immobilized on TiO2 NPs at concentration (0.3, 0.4, 0.5) mg/ml figure (7- D).

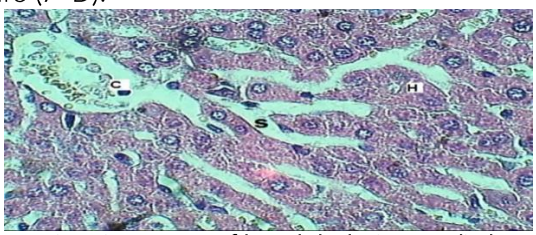

Figure (4- A): Section of liver lobule (Control) showed: Normal Central vein (C), hepatocyte (H), sinusoid (S). H&E stain.400x

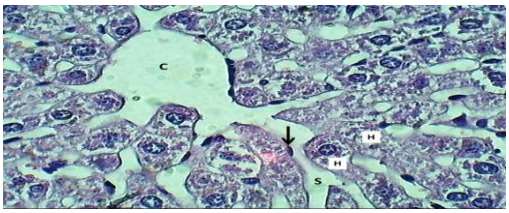

Figure (4- B): Section of liver lobule (elastase injection: 0.5 mg/ml) showed: normal appearance of central vein (C), hepatocyte (H), sinusoid (S) & kupffer cells (Arrow). H&E stain.400x

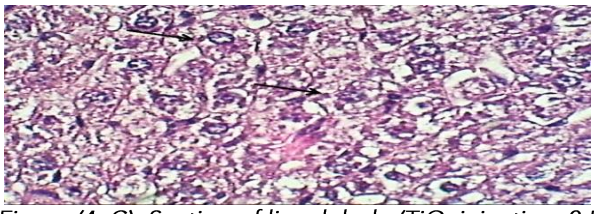

Figure (4- C): Section of liver lobule (TiO_2 injection: 0.5 mg/ml) showed mild cellular swelling of hepatocyte (Black arrows) which showed vacular degeneration (Arrows). H&E stain.400x

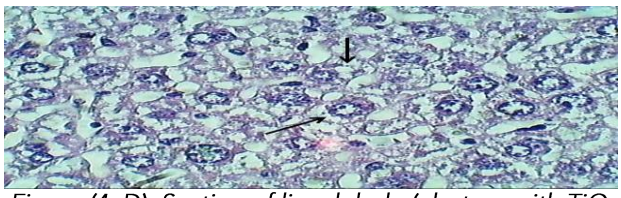

Figure (4- D): Section of liver lobule (elastase with TiO_2 injection: 0.4 mg/ml) showed moderate infiltration of lymphocytes (Red arrows), apoptosis (Black arrow) and vaculation of hepatocytes (Asterisk). H&E stain.400x

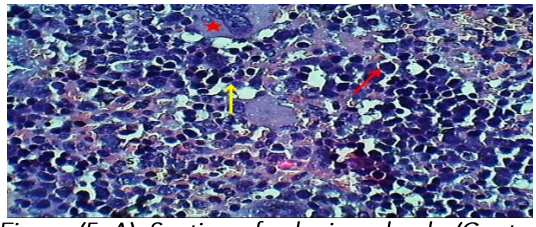

Figure (5- A): Section of splenic red pulp (Control group) shows: Normal lymphocyte (yellow arrow) macrophage (Red arrow), sinus (S) . H&E stain. 400x.

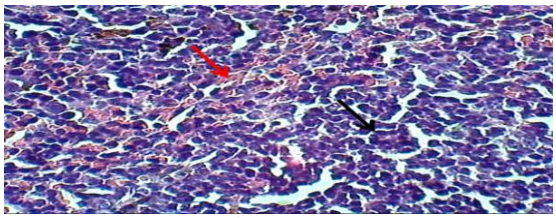

Figure (5- B): Section of spleen (elastase injection : 0.5) showed: normal white pulp (Wp) & Red pulp (Rp). H&E stain. 400x.

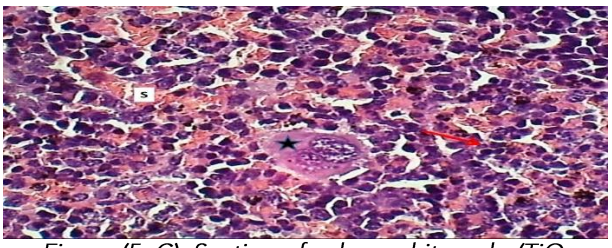

Figure (5- C): Section of spleen white pulp (TiO_2 injection: 0.5 mg/ml) showed: normal lymphocytes (Red arrow), sinusoids (S) and megakaryocytes (asterisk). H&E stain. 400x.

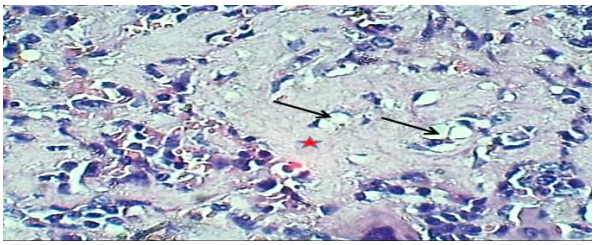

Figure (5- D): Section of spleen (elastase with TiO_2 injection:0.5 mg/ml) showed: vaculated lymphocytes (Arrows) & amyloid deposition (Asterisks). H&E stain. 400x.

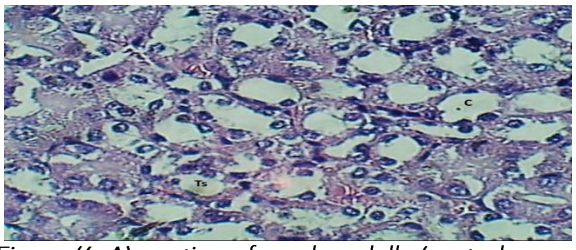

Figure (6- A): section of renal medulla (control group) showed: normal thick segment (Ts) and collecting renal tubule (C). H&E stain.400x

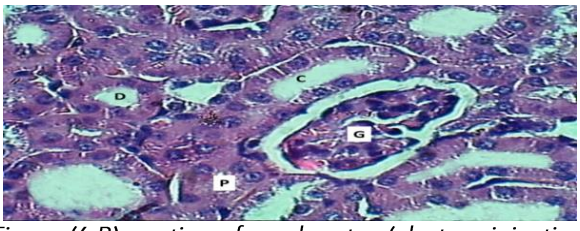

Figure (6-B): section of renal cortex (elastase injection: 0.5mg/ml) showed: normal glomeruli (G), collecting (C,) proximal (P) & distal convoluted tubules (D) . H&E stain.400x.

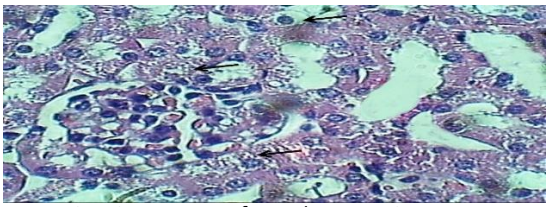

Figure (6-C): section of renal cortex (TiO_2 injection: 0.5mg/ml) showed: mild vacular and granular degeneration of epithelial cells of renal tubules (arrows). H&E stain.400x

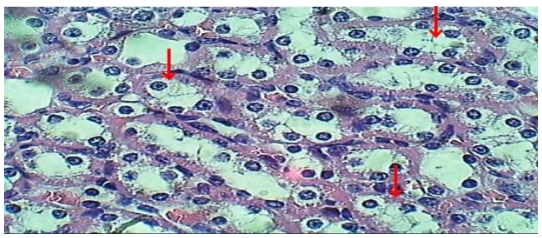

Figure (6- D): Section of renal medulla (elastase with TiO_2 injection: 0.5 mg/ml) showed: moderate vacular degeneration and swelling of epithelial renal tubules (arrows) with inter tubular vascular congestion . H&E stain.400x.

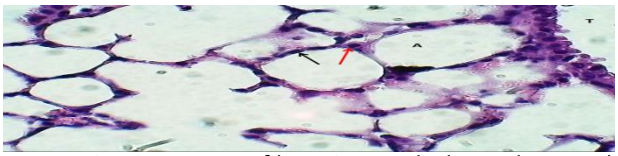

Figure (7-A): Section of lung (Control) showed: normal terminal bronchiole (T), alveolus (A) & pnumocyte-I (Red arrow) & type-II (Black arrow)).H&E stain.400x.

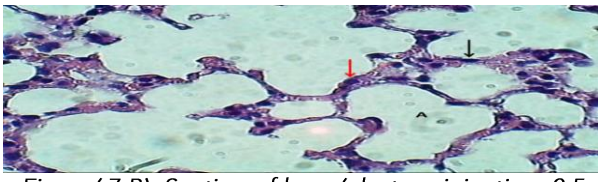

Figure(7-B): Section of lung (elastase injection: 0.5 mg/ml) showed: normal alveolus (A) & pnumocyte-I (Black arrow) & type-II (Red arrow).H&E stain.400x.

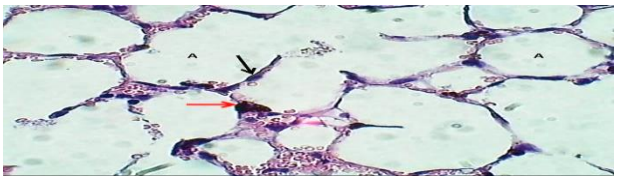

Figure (7-C): Section of lung (TiO_2 injection : 0.5 mg/ml) showed: normal alveolus (A) & pnumocyte-I (Black arrow) & type-II (Red arrow).H&E stain.400x.

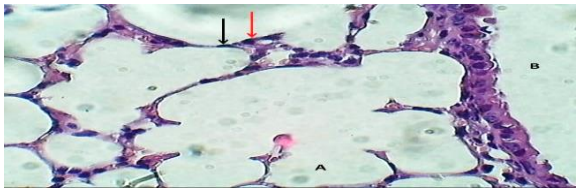

Figure (7- D): Section of lung (elastase with TiO_2 injection: 0.5 mg/ml) showed: normal bronchiole (B), alveolus (A) & pnumocyte-I (Black arrow) & type-II (Red arrow).H&E stain.400x.

Chen et al., (2009) showed that TiO2 particles were found to cause histological alterations in kidney. There was a slight enlargement in the renal glomerulus. Dilatation and proteinic liquids were also discovered in the renal tubules of mice exposed to TiO2 particles. While Wang et al., (2007) showed, the hydropic degeneration around the central vein was prominent in liver. This symptom did not appear in the mice exposed to 25 nm TiO2 nanoparticles.

4. Conclusion

The results of the present investigation showed that the klebsiella pneumoniae bacteria as source of elastase enzyme. High specific activity for elastase

purified from klebsiella pneumoniae (NJ22) is obtained purification. The enzyme characteristics were studied in terms of stability of activity within a range of pH, temperature, and the effect of inhibitors and salts. Elastase enzyme don't possess high cytotoxicity in vivo study. Free and immobilize elastase had cytotoxic activity against A375 lung cancer cell line. Five cellular parameters (VCC, NI, CMP, MMP,and cytochrome C), were studied after(24 hours) of exposures to free and immobilized enzyme.

Acknowledgment

The author would like to thank Al-Mustansiriyah University, Baghdad, Iraq (www.uomustansiriyah.edu.iq) for the support of this work.

References

Abbas, O. N., Mhawesh, A. A., & Al-Shaibani, A. B. (2020). Molecular identification of pathogenic klebsiella pneumoniae strains producing biofilm. *Medico-Legal Update*, *20*(3), 1068–1074. https://doi.org/10.37506/mlu.v20i3.1544

Abraham, V. C., Towne, D. L., Waring, J. F., Warrior, U., & Burns, D. J. (2008). Application of a high-content multiparameter cytotoxicity assay to prioritize compounds based on toxicity potential in humans. *Journal of Biomolecular Screening*, *13*(6), 527–537. https://doi.org/10.1177/1087057108318428

Ahmad, R., & Sardar, M. (2014). Immobilization of cellulase on TiO2 nanoparticles by physical and covalent methods: A comparative study. *Indian Journal of Biochemistry and Biophysics*, *51*(4), 314–320.

Al-Dulimi, A. G., Al-Saffar, A. Z., Sulaiman, G. M., Khalil, K. A. A., Khashan, K. S., Al-Shmgani, H. S. A., & Ahmed, E. M. (2020). Immobilization of L-asparaginase on gold nanoparticles for novel drug delivery approach as anti-cancer agent against human breast carcinoma cells. *Journal of Materials Research and Technology*, *9*(6), 15394–15411. https://doi.org/10.1016/j.jmrt.2020.10.021

Al-shukri, A. F., Al-marzook, F. A., Al-hammadi, N. A., & Mutlag, I. H. (2020). *Pharmacophore ANTITUMOR ACTIVITY OF ALKALOIDS EXTRACT FROM OPUNTIA POLYACANTHA PLANT USING HIGH CONTENT SCREENING TECHNIQUE (HCS). 11*(1), 129–135.

Bisswanger, H. (2014). Enzyme assays. *Perspectives in Science*, *1*(1–6), 41–55. https://doi.org/10.1016/j.pisc.2014.02.005

Calbo, E., & Garau, J. (2015). The changing epidemiology of hospital outbreaks due to ESBL-producing Klebsiella pneumoniae: The CTX-M-15 type consolidation. *Future Microbiology*, *10*(6), 1063–1075. https://doi.org/10.2217/fmb.15.22

Chen, J., Dong, X., Zhao, J., & Tang, G. (2009). In vivo acute toxicity of titanium dioxide nanoparticles to mice after intraperitoneal injection. *Journal of Applied Toxicology*, *29*(4), 330–337. https://doi.org/10.1002/jat.1414

Cookson, M. D., & Stirk, P. M. R. (2019). *济無No Title No Title No Title*. *1*(1), 42–48.

Cortés-Eslava, J., Gómez-Arroyo, S., Risueño, M. C., & Testillano, P. S. (2018). The effects of organophosphorus insecticides and heavy metals on DNA damage and programmed cell death in two plant models. *Environmental Pollution*, *240*, 77–86. https://doi.org/10.1016/j.envpol.2018.04.119

Crissman, J. W., Goodman, D. G., Hildebrandt, P. K., Maronpot, R. R., Prater, D. A., Riley, J. H., Seaman, W. J., & Thake, D. C. (2004). Best Practices Guideline: Toxicologic Histopathology. *Toxicologic Pathology*, *32*(1), 126–131. https://doi.org/10.1080/01926230490268756

Din, N. A. S., Lim, S. J., Maskat, M. Y., Abd Mutalib, S., & Zaini, N. A. M. (2021). Lactic acid separation and recovery from fermentation broth by ion-exchange resin: A review. *Bioresources and Bioprocessing*, *8*(1), 1–23.

Dong, Y. W., Liao, M. L., Meng, X. L., & Somero, G. N. (2018). Structural flexibility and protein adaptation to temperature: Molecular dynamics analysis of malate dehydrogenases of marine molluscs. *Proceedings of the National Academy of Sciences of the United States of America*, *115*(6), 1274–1279. https://doi.org/10.1073/pnas.1718910115

Everett, M. J., & Davies, D. T. (2021). Pseudomonas aeruginosa elastase (LasB) as a therapeutic target. *Drug Discovery Today*.

Fujii, T., Fukano, K., Hirano, K., Mimura, A., Terauchi, M., Etoh, S., & Iida, A. (2020). A new serine protease family with elastase activity is produced by Streptomyces bacteria. *Microbiology*, *166*(3), 253–261.

Heinz, A. (2020). Elastases and elastokines: elastin degradation and its significance in health and disease. *Critical Reviews in Biochemistry and Molecular Biology*, *55*(3), 252–273. https://doi.org/10.1080/10409238.2020.1768208

Hu, X., Li, D., Qiao, Y., Wang, X., Zhang, Q., Zhao, W., & Huang, L. (2020). Purification, characterization and anticancer activities of exopolysaccharide produced by Rhodococcus erythropolis HX-2. *International Journal of Biological Macromolecules*, *145*, 646–654. https://doi.org/10.1016/j.ijbiomac.2019.12.228

Karanam, G., & Arumugam, M. K. (2020). Reactive oxygen species generation and mitochondrial dysfunction for the initiation of apoptotic cell death in human hepatocellular carcinoma HepG2 cells by a cyclic dipeptide Cyclo(-Pro-Tyr). *Molecular Biology Reports*, *47*(5), 3347–3359. https://doi.org/10.1007/s11033-020-05407-5

Kotb, E., El-Zawahry, Y. A., & Saleh, G. E. (2019). Isolation of a putative virulence agent, cytotoxic serine-elastase, from a newly isolated Pseudomonas aeruginosa ZuhP13. *Journal of Biosciences*, *44*(1). https://doi.org/10.1007/s12038-018-9829-3

Kruchko, C., Gittleman, H., Ruhl, J., Hofferkamp, J., Ward, E. M., Ostrom, Q. T., Sherman, R. L., Jones, S.

F., Barnholtz-Sloan, J. S., & Wilson, R. J. (2019). Cancer collection efforts in the United States provide clinically relevant data on all primary brain and other CNS tumors. *Neuro-Oncology Practice*, *6*(5), 330–339. https://doi.org/10.1093/nop/npz029

Lei, Y., Zhao, P., Li, C., Zhao, H., Shan, Z., & Wu, Q. (2018). Isolation, identification and characterization of a novel elastase from Chryseobacterium indologenes. *Applied Biological Chemistry*, *61*(3), 365–372. https://doi.org/10.1007/s13765-018-0364-6

Li, J., Ramezanpour, M., Fong, S. A., Cooksley, C., Murphy, J., Suzuki, M., Psaltis, A. J., Wormald, P. J., & Vreugde, S. (2019). Pseudomonas aeruginosa Exoprotein-Induced Barrier Disruption Correlates With Elastase Activity and Marks Chronic Rhinosinusitis Severity. *Frontiers in Cellular and Infection Microbiology*, *9*(February), 1–9. https://doi.org/10.3389/fcimb.2019.00038

Lin, X., Xu, W., Huang, K., Mei, X., Liang, Z., Li, Z., Guo, J., & Luo, Y. B. (2009). Cloning, expression and characterization of recombinant elastase from Pseudomonas aeruginosa in Picha pastoris. *Protein Expression and Purification*, *63*(2), 69–74. https://doi.org/10.1016/j.pep.2007.12.011

Logan, P. G. B. and G. D. (2014). 基因的改变NIH Public Access. *Bone*, *23*(1), 1–7. https://www.ncbi.nlm.nih.gov/pmc/articles/PMC3624763/pdf/nihms412728.pdf

Ma, X., Hartmann, R., Jimenez De Aberasturi, D., Yang, F., Soenen, S. J. H., Manshian, B. B., Franz, J., Valdeperez, D., Pelaz, B., Feliu, N., Hampp, N., Riethmüller, C., Vieker, H., Frese, N., Gölzhäuser, A., Simonich, M., Tanguay, R. L., Liang, X. J., & Parak, W. J. (2017). Colloidal Gold Nanoparticles Induce Changes in Cellular and Subcellular Morphology. *ACS Nano*, *11*(8), 7807–7820. https://doi.org/10.1021/acsnano.7b01760

Meryam Sardar, R. A. (2015). Enzyme Immobilization: An Overview on Nanoparticles as Immobilization Matrix. *Biochemistry & Analytical Biochemistry*, *04*(02). https://doi.org/10.4172/2161-1009.1000178

Mukherjee, G., & Banerjee, R. (2006). Effects of temperature, pH and additives on the activity of tannase produced by a co-culture of Rhizopus oryzae and Aspergillus foetidus. *World Journal of Microbiology and Biotechnology*, *22*(3), 207–212. https://doi.org/10.1007/s11274-005-9022-3

Patel, S. S., Chauhan, H. C., Patel, A. C., Shrimali, M. D., Patel, K. B., Prajapati, B. I., Kala, J. K., Patel, M. G., rajgor, M., & Patel, M. A. (2017). Isolation and Identification of Klebsiella pneumoniae from Sheep-Case Report. *International Journal of Current Microbiology and Applied Sciences*, *6*(5), 331–334. https://doi.org/10.20546/ijcmas.2017.605.037

Povoa, L. V., Calvi, U. C. B., Lorena, A. C., Ribeiro, C. H. C., & Da Silva, I. T. (2021). A Multi-Learning Training Approach for Distinguishing Low and High Risk Cancer Patients. *IEEE Access*, *9*, 115453–115465. https://doi.org/10.1109/ACCESS.2021.3104820

Ranjit, R. (2010). A primer on the Taguchi method: Society of Manufacturing Engineers. *Estados Unidos: Society of Manufacturing Engineers*, 172–174.

Shinji, T., Moe, Y., Yukihiro, K., Yoko, Y., & Hitoshi, A. (2019). Characterization of an organic-solvent-stable elastase from Pseudomonas indica and its potential use in eggshell membrane hydrolysis. *Process Biochemistry*, *85*(June), 156–163. https://doi.org/10.1016/j.procbio.2019.06.021

Simard, M., Hill, L. A., Underhill, C. M., Keller, B. O., Villanueva, I., Hancock, R. E. W., & Hammond, G. L. (2014). Pseudomonas aeruginosa elastase disrupts the cortisol-binding activity of corticosteroid-binding globulin. *Endocrinology*, *155*(8), 2900–2908. https://doi.org/10.1210/en.2014-1055

Vasaikar, S., Obi, L., Morobe, I., & Bisi-Johnson, M. (2017). Molecular characteristics and antibiotic resistance profiles of klebsiella isolates in mthatha, eastern cape province, South Africa. *International Journal of Microbiology*, *2017*. https://doi.org/10.1155/2017/8486742

Wang, J., Zhou, G., Chen, C., Yu, H., Wang, T., Ma, Y., Jia, G., Gao, Y., Li, B., Sun, J., Li, Y., Jiao, F., Zhao, Y., & Chai, Z. (2007). Acute toxicity and biodistribution of different sized titanium dioxide particles in mice after oral administration. *Toxicology Letters*, *168*(2), 176–185. https://doi.org/10.1016/j.toxlet.2006.12.001

Yu, V. L., Hansen, D. S., Wen, C. K., Sagnimeni, A., Klugman, K. P., Von Gottberg, A., Goossens, H., Wagener, M. M., Benedi, V. J., Casellas, J. M., Trenholme, G., McCormack, J., Mohapatra, S., & Mulazimoglu, L. (2007). Virulence characteristics of Klebsiella and clinical manifestations of K. pneumoniae bloodstream infections. *Emerging Infectious Diseases*, *13*(7), 986–993. https://doi.org/10.3201/eid1307.070187